MEAN WIND AND TURBULENCE CHARACTERISTICS DUE TO INDUCTION EFFECTS NEAR WIND TURBINE ROTORS

David E. Neff
Robert N. Meroney

Fluid Mechanics and Wind Engineering Program
Department of Civil Engineering
Colorado State University
Fort Collins, CO 80523

for

Third International Colloquium on
BLUFF BODY AERODYNAMICS AND ITS APPLICATIONS, BBAA III

Virginia Polytechnic Institute
Blacksburg, Virginia
July 28 - August 1, 1996

MEAN WIND AND TURBULENCE CHARACTERISTICS DUE TO INDUCTION EFFECTS NEAR WIND TURBINE ROTORS

David E. Neff, Research Scientist
Robert N. Meroney, Professor
Fluid Mechanics and Wind Engineering Program
Civil Engineering Department, Colorado State University
Fort Collins, CO 80523

INTRODUCTION

Aerodynamicists currently use wind field and turbulence information to calculate the character of dynamic loading that large wind-generator rotors receive.[4, 6, 7, 8] Unfortunately, these turbulence scales and intensities may be distorted by the pressure of the rotor flow field before they actually interact with the rotor blades. Indeed, wind-generator induction effects and streamline divergence caused by the hub and tower may significantly distort free wind field values. In recent years, a limited number of model and field scale measurement studies have examined near- and far-field turbine rotor wakes. [1, 5, 10] These wake studies were made to evaluate the influence of upwind turbines on downwind installations; little information appears in the literature concerning possible induction effects. It is the purpose of this paper to provide experimental model data on the wind field surrounding a single wind turbine rotor disk. These data should provide an improved physical insight into the induction effects of the air flow as it approaches the wind turbine. This insight should in turn improve an analytical model's predictive capabilities.

A scaled model of a horizontal axis wind turbine (a two bladed rotor of diameter 53 cm) was placed into the Meteorological Wind Tunnel (MWT) facility at Colorado State University. Four different approach flow conditions were studied; low and moderate turbulence levels (0.1% and 1.5% intensity) at both 6 and 7.6 m/s free stream air velocities. For each of these flow conditions the rotor power coefficient vs. tip speed ratio was obtained, and the 3-dimensional velocity field from 3 rotor diameters upwind to ½ diameter downwind was tabulated.

DATA ACQUISITION AND ANALYSIS

Laboratory measurement techniques are discussed in this section. Some of the methods used are conventional and need little elaboration.

Wind Tunnel Facility

The experiments were performed in the Meteorological Wind Tunnel (MWT) at

Colorado State University. This tunnel has a wind speed range of 0.3 to 30 m/s. The approach flow turbulent intensity varies upward from 0.1% . The test section in which the model wind turbine was located had a cross-sectional area of 3.34 m^2 (1.83m x 1.83m). The model was located 7 meters downwind from the convergent entrance to the test section. For the grid turbulence tests (turbulent intensity 1.5%) a dowel grid was mounted at the test section entrance. The dowels were 1.27 cm in diameter and spaced 12 cm apart. The wind turbine was placed in the spatially uniform velocity field downwind of the entrance.

Wind Turbine Model

The wind turbine model was built by Mr. Peter Bushnell of Cornell University [2, 3]. Figure 1 displays the mounting arrangement of this horizontal axis wind turbine .The rotor shaft is mounted on two support rods, each rod holds a low friction roller bearing to ensure rotor shaft rotational freedom. At the downwind end of the rotor shaft is mounted a small DC generator. A calibration of the generator's voltage variation versus rotational speed (obtained through the use of a strobe light) yielded the conversion equation rpm = 744 x (volts). The rotor diameter was 53.4 cm. The rotor blades were made of balsa wood covered with epoxy. The blade shape was that of a NACA 4415 airfoil section. A steel pin at the base of each blade was connected to the hub with a set screw, and the hub was also connected to the rotor shaft with set screws. The blade chord was constant (4.76 cm) over the entire length, the tips were cut square. The wind turbine was designed to operate at 1400 rpm, with a tip speed ratio of 5 and a lift coefficient of 1.0. The effective wind tunnel blockage presented by a spinning rotor disk was 4 % .

The power output of the rotor was obtained via a simple prony brake friction device that imparts a torque (measured by the deflection of a spring) to the spinning shaft of the wind turbine. The rotor speed, measured by a strobe light, was observed to vary with load from 900 rpm up to 2100 rpm for the flow conditions studied. The prony brake consisted of a spring mounted next to a ruler, a leather friction belt, an aluminum brake drum mounted on the rotor shaft, and a weight bucket. To start the wind turbine spinning one manually lifts the brake assembly away from the brake drum until the turbine reaches a rotational speed above its resonant frequency of around 1000 rpm. Once above this speed the prony brake is set back in place on the brake drum. The amount of weight placed in the bucket determines the rotor speed.

Flow Visualization Techniques

Video movies (VHS) were taken of helium soap bubbles produced by a Sage Bubble Generator as they floated through or by the spinning rotor blades. Video movies were also taken of a smoke plume produced by titanium tetrachloride as it flowed past by the rotor blades.

Velocity Measurements

Velocity measurements were made with pitot probes, single hot films, cross films and

three dimensional hot film systems. Pitot-static probes were used as a velocity standard during the calibration of the different hot film systems and to provide the reference upwind velocity measurement. Single-hot-film (TSI 1210 Sensor) measurements were used to document the longitudinal turbulence levels for the four different approach flow conditions and as an error estimator for the cross film and 3-d film measurements. Cross-film (TSI 1241) measurements were used to document the lateral and vertical turbulent level for one approach flow condition and as an error estimator for the 3-d hot film measurements.

A Thermo-System Incorporated (TSI) model 1294-20 3-dimensional hot-film probe was used for all measurements behind and to the side of the wind turbine. A specially made probe, similar to the TSI 1294-20 but with a 90 0 bend in the probe shaft 3.8 cm back from the sensors, was used for all measurements upwind of the wind turbine. The data reduction scheme use was similar to that described in TSI Technical Bulletin 8. The TSI model 1294-20 probe has three orthogonally-mounted, cylindrical hot films, (Diameter = 0.051 mm) each doubly supported (Figure 2). The probe can measure total vector velocities that are contained within the single octant defined by the three film positions. The transducer response was directed to an analog to digital converter connected to an HP-1000 mini-computer system for on-line data reduction. The statistical values computed from the u-v-w time series in axisymmetrical coordinates for each position are:

1) Mean, rms, skewness, and flatness of the axial velocity component,
2) Mean, rms, skewness, and flatness of the radial velocity component,
3) Mean, rms, skewness, and flatness of the angular velocity component,
4) Mean velocity vectors angles from the axial, radial and angular coordinate directions,
5) Reynolds stresses,
6) Mean, rms, skewness, and flatness of the angular deviations about the axial axis,
7) Mean, rms, skewness, and flatness of the angular deviations about the radial axis, and
8) Mean, rms, skewness. and flatness of the angular deviations about the angular axis.

TEST PROGRAM AND DATA

The test program consisted of documenting the different approach flow characteristics, measurement of the performance (power coefficient vs. tip speed ratio) of the model wind turbine, and the tabulation of the flow field near the spinning rotor. The approach flow was uniform and steady (within +2%) over the center portion of the wind tunnel. The moderate turbulence cases were produced by the placement of a grid at the entrance of the test section. Measurements were performed for approach flow characterized by mean wind speeds of 6, 7.6 and 7.6 m/s and turbulence levels of 0.1, 0.1 and 1.5 %, respectively. Three dimensional velocity measurements were taken at 58 spatial locations upwind, downwind and to the side of the rotor. All turbulence characteristics were defined from time series taken at a digital sampling rate of 1563 Hz for a total of 32384 samples. Given a rotor speed of approximately 1400 rpm, the velocity time series includes about 967 passes of the rotor blade, or 67 samples were taken for every revolution of the rotor or every 5.37 degrees of blade rotation. These sample conditions were of sufficient length to insure an accuracy of ±5 % in the computation of the mean, rms, and flatness. [9]

DISCUSSION

Visualization Results

When helium soap bubbles were introduced into flow upwind of the spinning rotor three different phenomena were observed. 1) Most bubbles passed through the spinning rotor and were then caught up in the counter swirling flow downwind of the rotor. That is the rotor was spinning in a counterclockwise sense, the flow downwind of the rotor swirled in a clockwise sense. This result was expected due to the conservation of angular momentum for this system. 2) When the bubble source was placed at approximately 3/4 of a radius from the hub most bubbles seemed to have a straight line approach to the spinning rotor; nonetheless, roughly around 20 % of them were deflected angularly before reaching the rotor plane. This deflection appeared to be fairly abrupt and occurred around 1/4 to ½ a rotor radius upwind. 3) When bubbles were caught up into the tip vortices these vortices appear to be quite tight with a bubble making a full revolution in the equivalent distance of approximately one blade length. The visual results from introducing a smoke source upwind of the rotor was not able to reproduce the detailed flow seen by observing helium soap bubbles but it did display the curving of streamlines radially outward around the spinning rotor blades. This is a demonstration of the existence of axial induction effects.

Wind Field Results

Figure 3 displays the normalized mean axial velocity change $100 \times (u_x - (u_x)_\infty)/(u_x)_\infty$ versus axial distance in rotor diameters for U = 7.6 m/sec and T.I. = 0.1 %. The figure shows that the axial component of flow approaching the rotor disk was decelerated in a core region defined by a tube containing the rotor disk and accelerated outside this region. This deceleration was reasonably uniform with radial position up to the measurement location just upwind of the rotor (1/8 rotor diameter). Then it radically departs from this trend as the flow passes through the rotor. An axial induction factor based on mean velocity measurements at 1/8 rotor diameter upwind would be 0.125 but depending on how one extrapolates the data through the rotor section, a radially depended axial induction factor may vary from 0.125 to 0.42. The flow outside of the rotor tube accelerates as was expected from mass continuity. The ordering of velocity magnitudes with radial distance take an unexplained reversal as the flow passes outside of the rotor blades. The estimation of axial induction factors based on mean velocity values may be in error due to the transient nature of velocity values as the rotor blade passes. The axial velocity just upwind of the rotor varies in a roughly sinusoidal form about its mean value. The periodic variation of axial flow velocity may be as large as +7.5% of the mean value at 118 rotor diameters upwind. If the minimum velocity value were used rather than the mean the computed axial induction factor would be 0.2 instead of 0.133. Thus the transient nature of the flow has a significant influence on values important to the aerodynamic performance of the wind turbine.

Comparison between plots with similar approach velocities but different turbulence levels do not show any major flow differences in this format. Comparison between plots with similar turbulence levels but different approach velocities display a difference in the magnitude

of the range of mean axial velocities in the wake region of the turbine only. The range of axial velocity variation was greatest in the lower approach wind speed cases.

Figure 4 displays the normalized mean radial velocity 100 x u_R /$(u_x)_\infty$ versus axial distance in rotor diameters for the same approach flow conditions. It shows that the flow was divergent approaching the wind turbine and in the wake region out to at least one-half rotor diameters downwind. The maximum divergence is at the rotor disk where the mean velocity vector deviated by 10^0 from that of the approach flow. The radial velocities are greatest (14-20% of the approach velocity value) near the tip region. The radial velocity transient variation just upwind of the disk and downwind outside of the rotor wake are nearly sinusoidal in form as observed by a flatness factor near to 1.5.

Figure 5 displays the normalized mean angular velocity 100 x $u_\theta/(u_x)_\infty$ versus axial distance in rotor diameters. Within the wake region large negative angular velocities exist (the rotor was spinning in the positive sense). The magnitude of these angular velocities was greatest (≈25% of the approach flow velocity) at the inner most radial measurement position of one-eighth rotor diameter. The flow immediately upwind of the rotor and the flow downwind of the rotor but outside of its wake have negative mean angular velocities, but their magnitude (≈2-3% of the approach flow velocity) is much less than that in the wake region.

Classical vortex/strip theory assumes that the angular velocity at the rotor disk is one-half the angular velocity imparted to the slip stream. [11] This assumption leads to the use of an angular induction factor, a', to correct blade section angle of attack for induced rotational motions. These corrections usually presume a rotating activator disk with an infinite number of blades. To compute the instantaneous angular induction factor for the model wind turbine a correlation between the rotor blades position and the angular velocity components magnitude must be known, unfortunately, a blade position time series was not measured during this study. Examination of the axial and angular velocity time series can give a qualitative estimate as to the sign of the angular induction factor. The sharp drop seen in the axial velocity time series is undoubtably due to the pressure field surrounding a passing rotor blade. This fall in axial velocity occurs at the same time as a sharp maximum in the angular velocity time series. This would indicate that the rotor blade sees an angular velocity component that is in the opposite direction to the rotor blade travel.

Figure 6 displays the axial turbulent intensity 100 x (u_x)rms/$(u_x)_\infty$ versus axial distance in rotor diameters. It shows that the axial turbulent intensity increases dramatically in the region approaching the rotor disk and then decrease sharply again in the rotor wake. The sharp increase in turbulent intensity for the spacial location of X = ½, R = 1/8 is due to the influence of the growing wake caused by the wind turbines hub and support mechanism. Plots of the axial flatness factor versus axial distance show that most of this turbulent intensity in the non-wake region is due to an organized periodic structure of slowly varying amplitudes, approaching that of a sine wave.

The velocity time series for the axial velocity component and the angular velocity component help estimate the angle of attack during a rotor cycle. The rotor rotational

velocity, 25.81 rps, was estimated by measuring the time period between blade passages. At a radius of 0.201 m the velocity of this rotor blade section, was 32.6 m/s. This information was used to plot the angle of attack time series. The periodic nature of axial induction is the primary cause for variations in the angle of attack for this approach flow and position.

REFERENCES

1. Baker, Robert W. and Stel N. Walker. (1982) "Wake Studies at the Goodnoe Hills Mod-2 Site". DOE/BP-182, Bonneville Power Administration, Oregon State University, pp. 1-89.
2. Bushnell, P. "Design of Rotor Blades for a Model Horizontal Axis Wind Turbine". Cornell University, May 1984.
3. Bushnell, P. "Experimental Study of the Vortex Wake Formed by a Model Wind Turbine". Cornell University, December 1983.
4. Cliff, W.C. and G.H. Fichtl. (1978) "Wind Velocity-Change (Gust Rise) Criteria for Wind Turbine Design". PNL-2526, U.S. Department of Energy, Pacific Northwest Laboratory, pp. 1-17.
5. Eberle, W.R. (1981) "Wind Flow Characteristics in the Wakes of Large Wind Turbines". DOE/NASA0029-1, U.S. Department of Energy, Lockheed Missiles and Space Company, Inc., pp. 1-211.
6. Fichtl, G. (1983) "Covariance Statistics of Turbulence Velocity Components for Wind Energy Conversion System Design-Homogeneous, Isotropic Case". PNL-3499, Department of Energy, Pacific Northwest Laboratory, PP. 1-53.
7. Hansen, A. Craig. (1979) "Effects of Turbulence on Wind Turbine Performance". ASCE Reprint 3537, pp. 1-17.
8. Kareem, A. (1981) "Wind-Loading Definition for the Structural Design of Wind-Turbine Generators". *Journal of Energy*, Vol. 5, No. 2, pp. 89-93.
9. Neff, D.E. and Meroney, R.N. (1987), "Measurement in a Wind Tunnel of the Modification of Mean Wind and Turbulence Characteristics Due to Induction Effects Near Wind Rotors," Battelle Pacific Northwest Laboratory Report PNL-6248 , 145 pp.
10. Riley, James, J. , Geller, Edward W. , Coon, Max D. , and Schedvin, John C. (1980) "A Review of Wind Turbine Wake Effects". DOE/ET/23160-80/1, U.S. Department of Energy, Flow Research Company, pp. 1-118.
11. Wilson, R.E., Lissaman, P.B.S., and Walker, S.N. "Aerodynamic Performance of Wind Turbines". Oregon State University, p. 164, June 1976.

ACKNOWLEDGMENTS

Financial support from the U.S. Department of Energy through a grant from Battelle, Pacific Northwest Laboratories is gratefully acknowledged. Advice and suggestions during the measurement program and data analysis activities from Drs. R. Connell, R.W. Thresher and N.D. Kelley are appreciated.

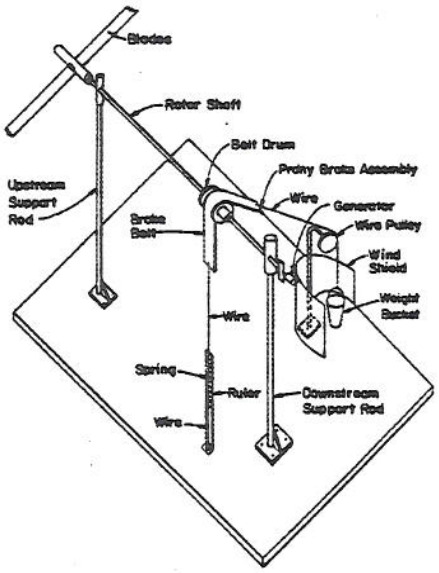

Figure 1 Model wind turbine and Prony brake

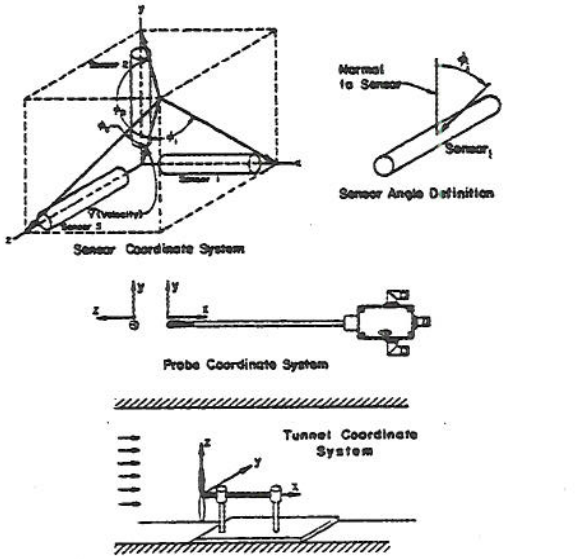

Figure 2 Sensor, probe and tunnel coordiate system

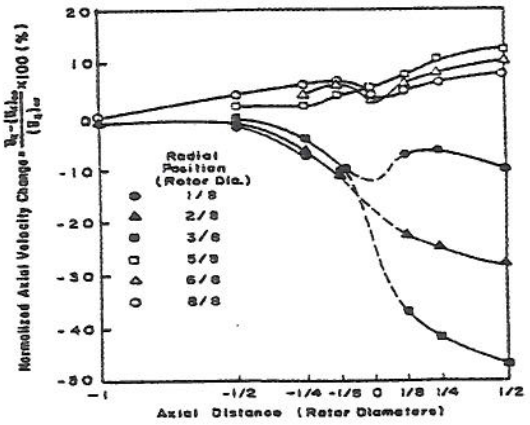

Figure 3 Normalized mean axial velocity change vs. axial distance for U = 7.6 m/s, T.I. = 0.1%

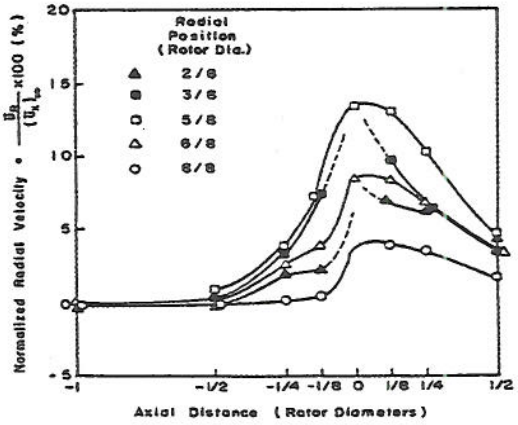

Figure 4 Normalized mean radial velocity change vs. axial distance for U = 7.6 m/s, T.I. = 0.1%

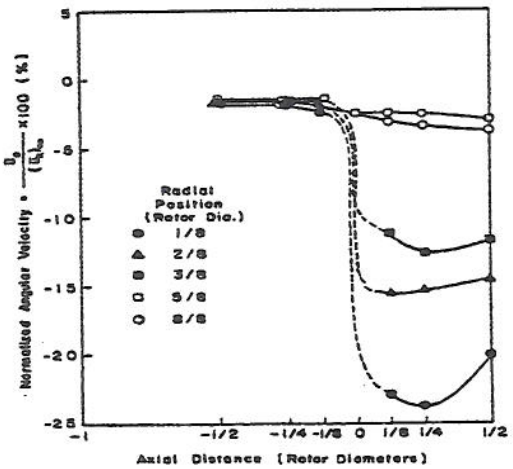

Figure 5 Normalized mean angular velocity change vs. axial distance for U = 7.6 m/s, T.I. = 0.1%

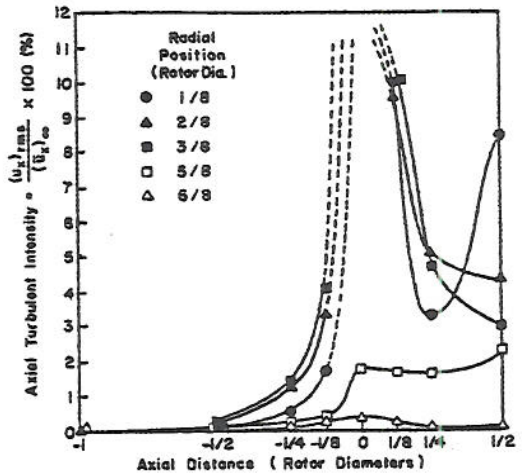

Figure 6 Axial turbulence intensity vs. axial distance for U = 7.6 m/s, T.I. = 0.1%

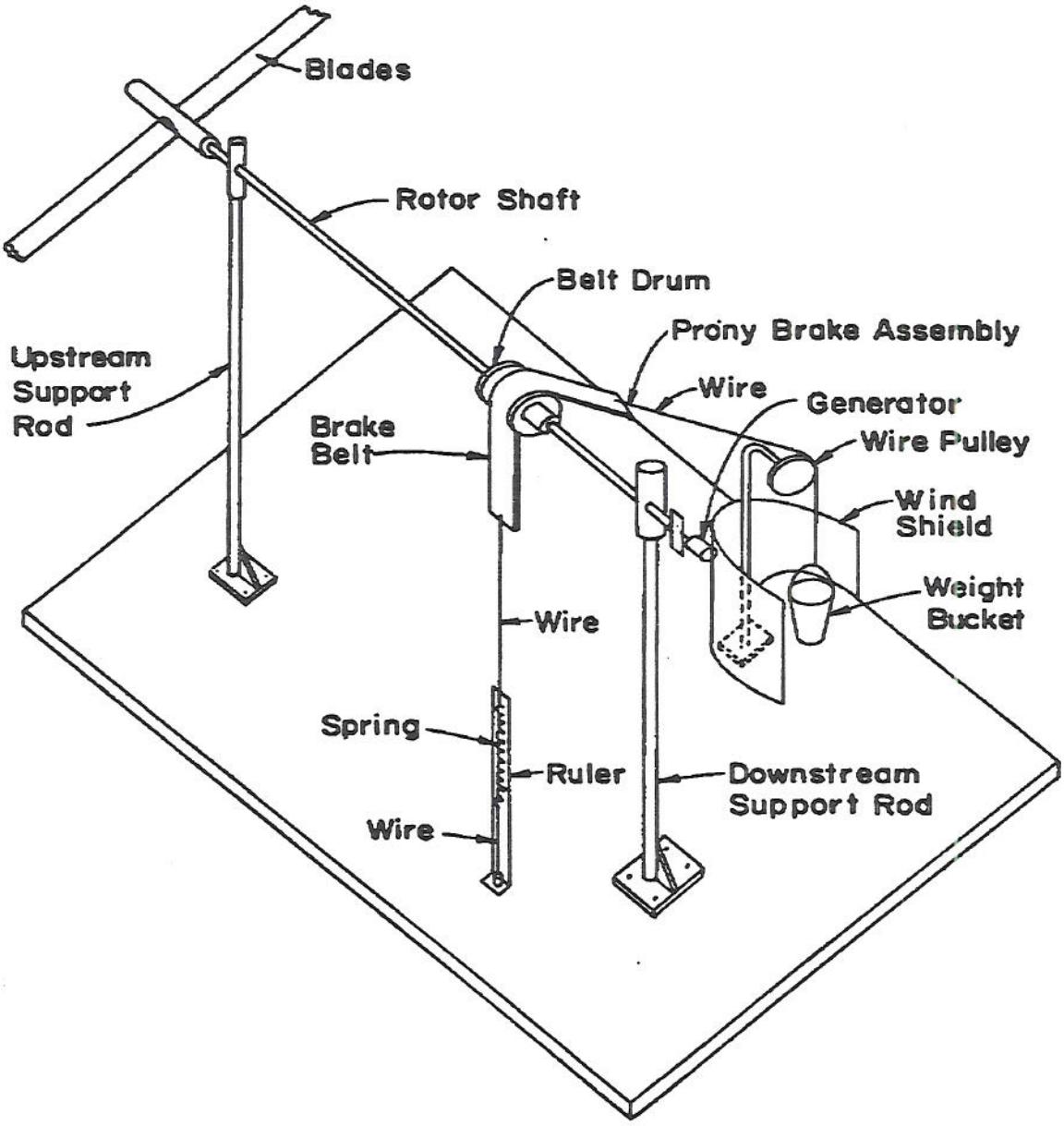

Figure 1 Model wind turbine and Prony brake

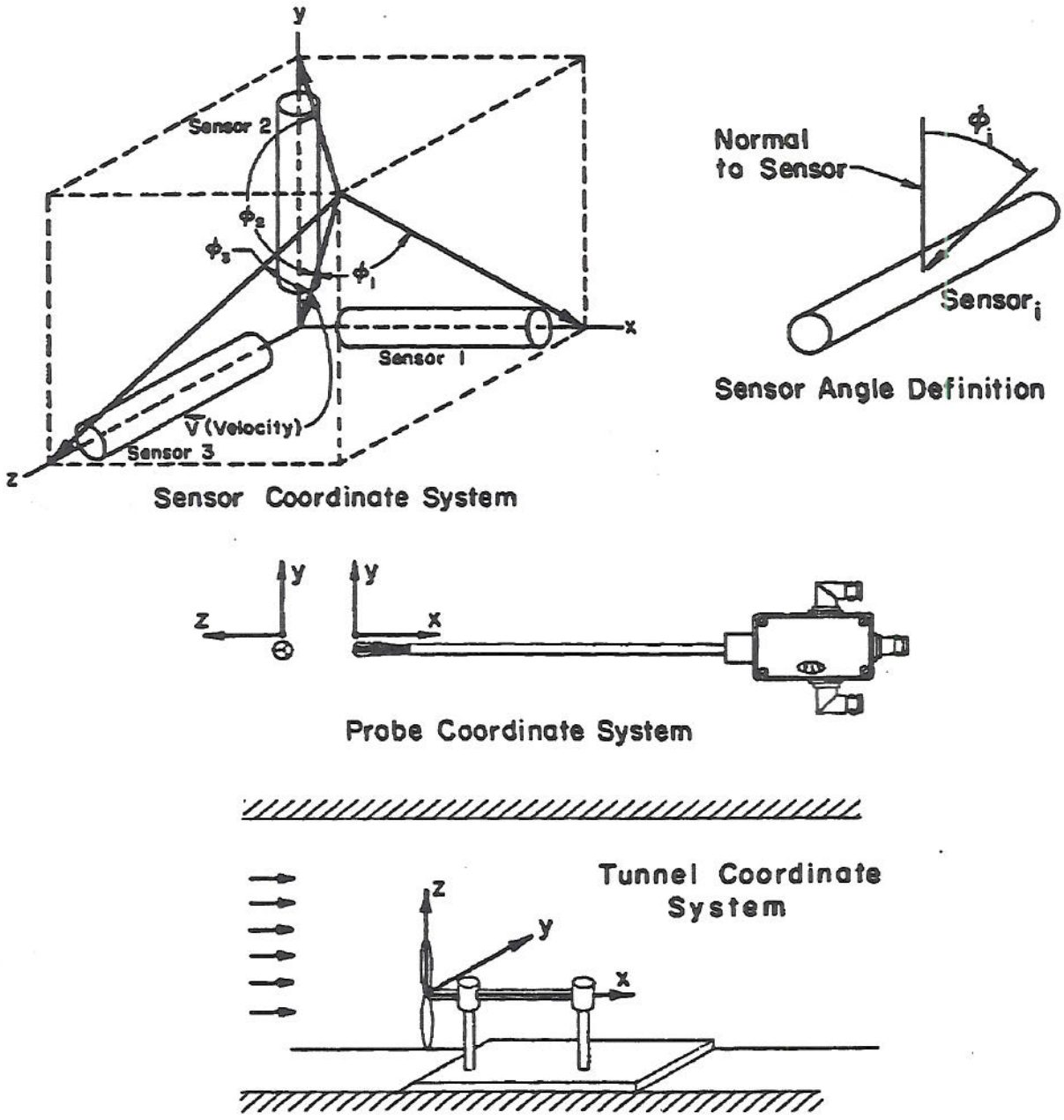

Figure 2 Sensor, probe and tunnel coordiate system

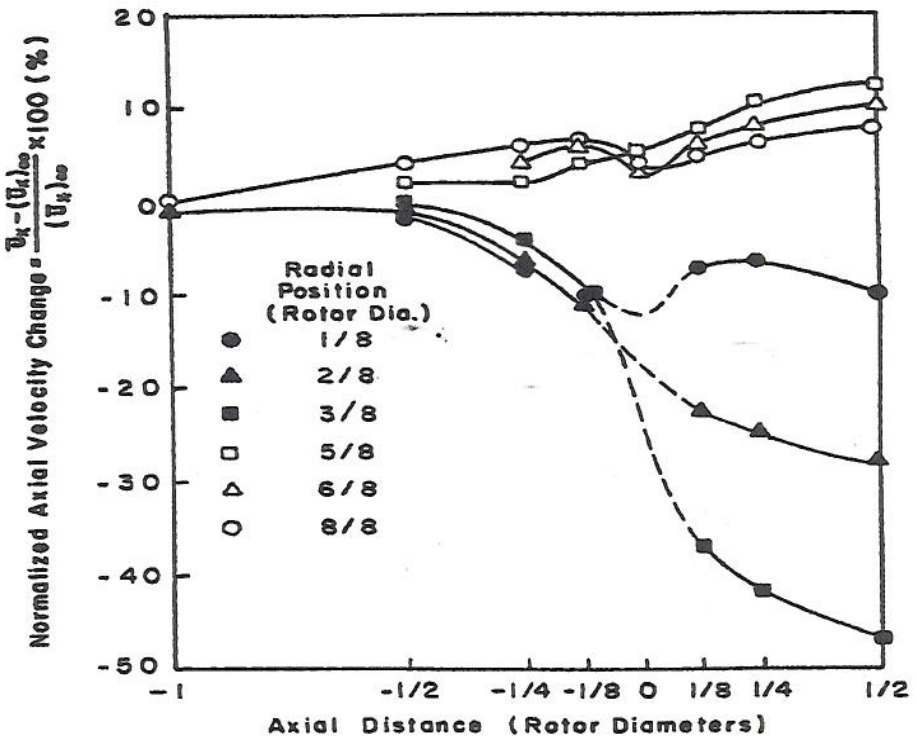

Figure 3 Normalized mean axial velocity change vs. axial distance for U = 7.6 m/s, T.I. = 0.1%

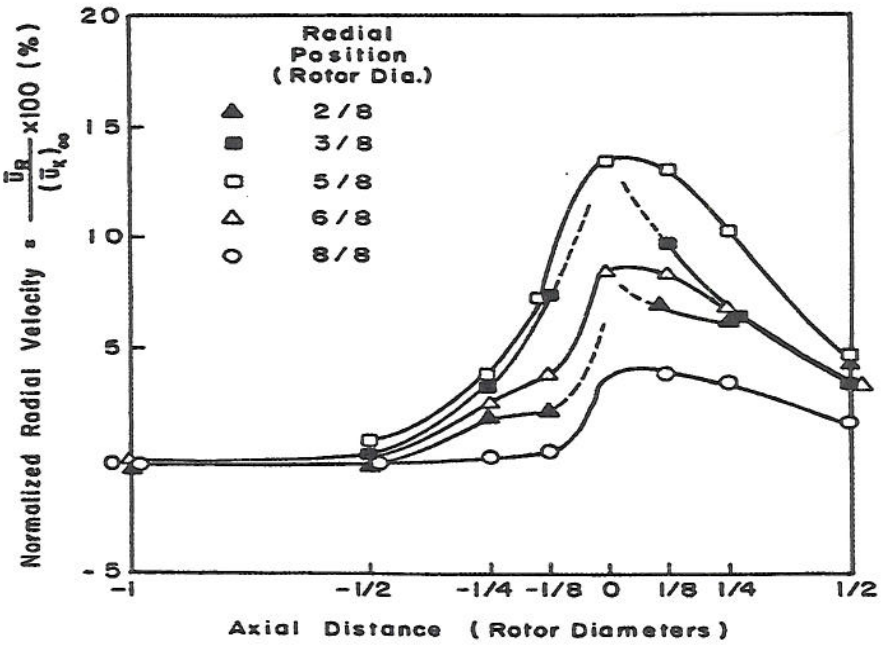

Figure 4 Normalized mean radial velocity change vs. axial distance for U = 7.6 m/s, T.I. = 0.1%

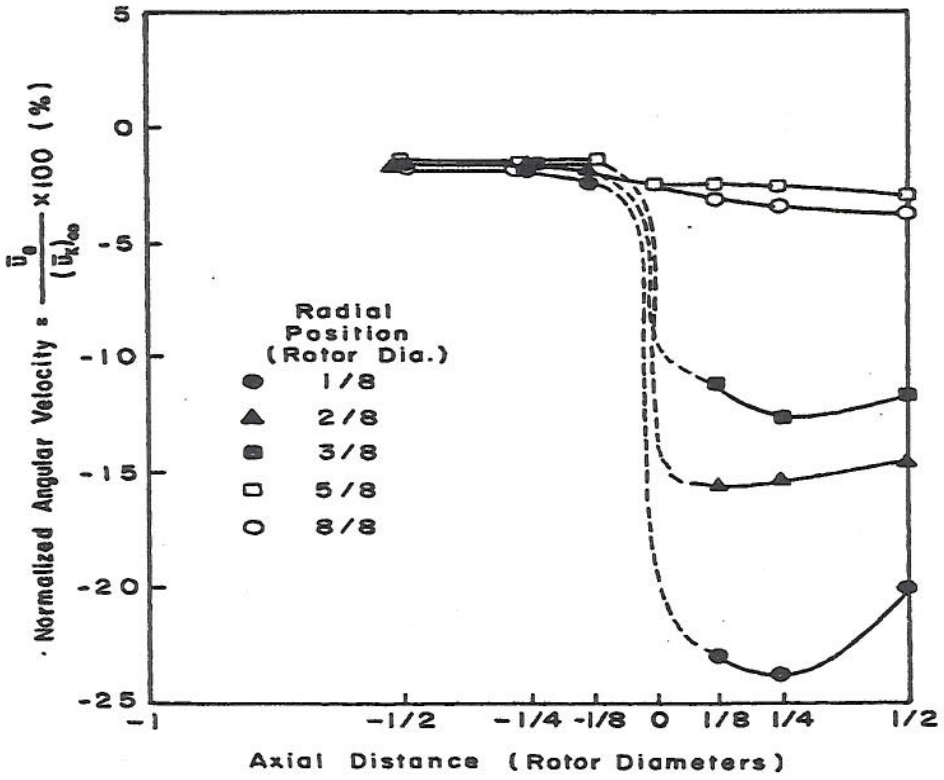

Figure 5 Normalized mean angular velocity change vs. axial distance for U = 7.6 m/s, T.I. = 0.1%

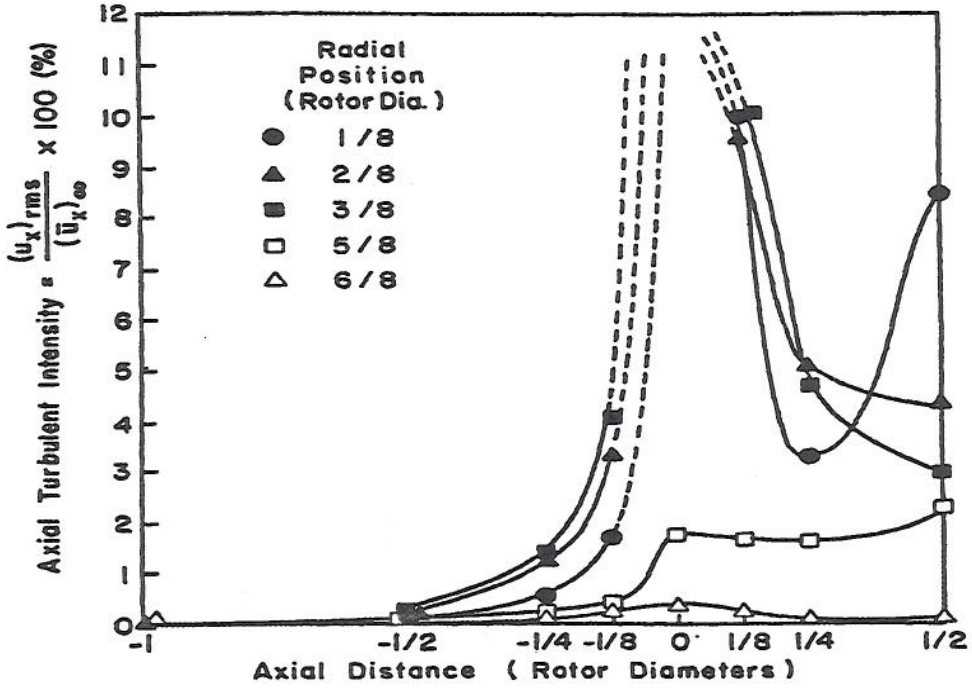

Figure 6 Axial turbulence intensity vs. axial distance for U = 7.6 m/s, T.I. = 0.1%

MEAN WIND AND TURBULENCE CHARACTERISTICS DUE TO INDUCTION EFFECTS NEAR WIND TURBINE ROTORS

David E. Neff
Robert N. Meroney

Fluid Mechanics and Wind Engineering Program
Department of Civil Engineering
Colorado State University
Fort Collins, CO 80523

for

Third International Colloquium on
BLUFF BODY AERODYNAMICS AND ITS APPLICATIONS, BBAA III

Virginia Polytechnic Institute
Blacksburg, Virginia
July 28 - August 1, 1996

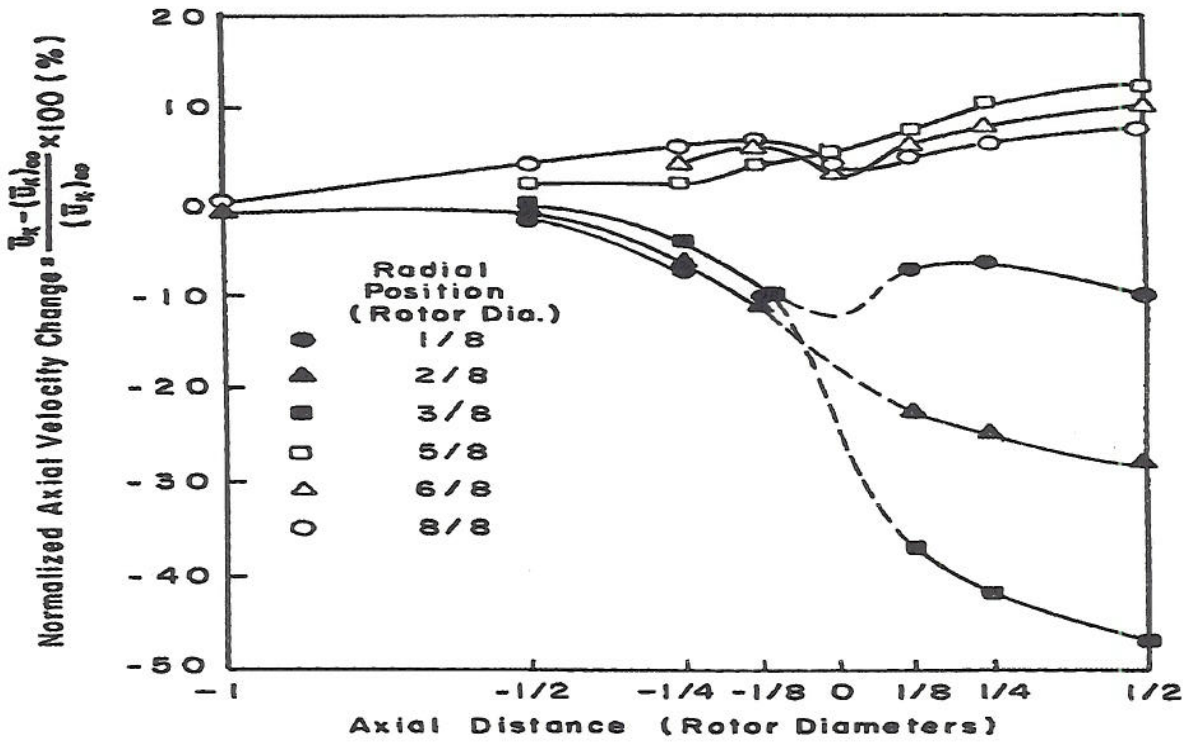

Figure 3 Normalized mean axial velocity change vs. axial distance for U = 7.6 m/s, T.I. = 0.1%

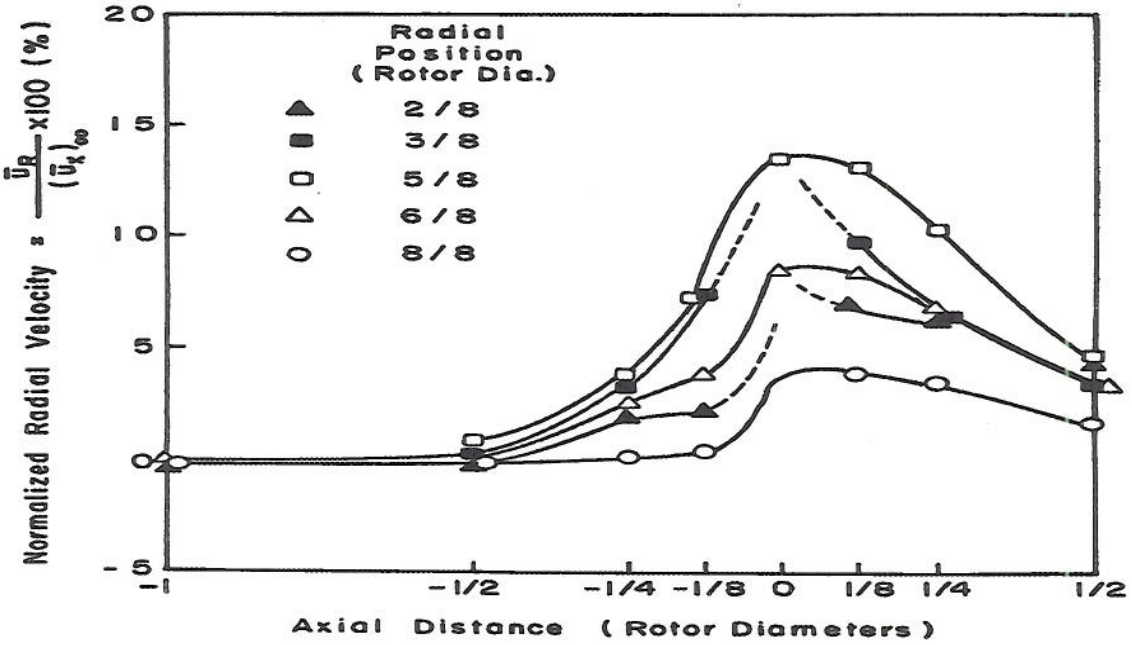

Figure 4 Normalized mean radial velocity change vs. axial distance for U = 7.6 m/s, T.I. = 0.1%

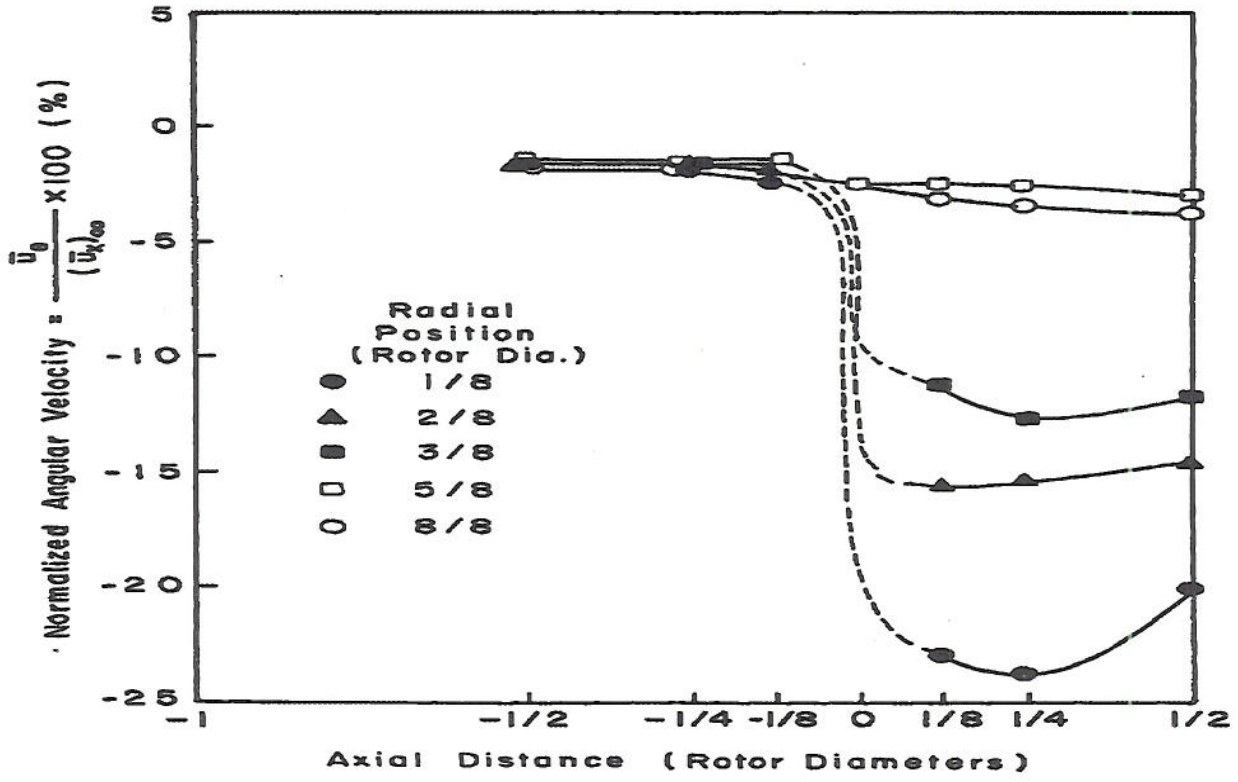

Figure 5 Normalized mean angular velocity change vs. axial distance for U = 7.6 m/s, T.I. = 0.1%

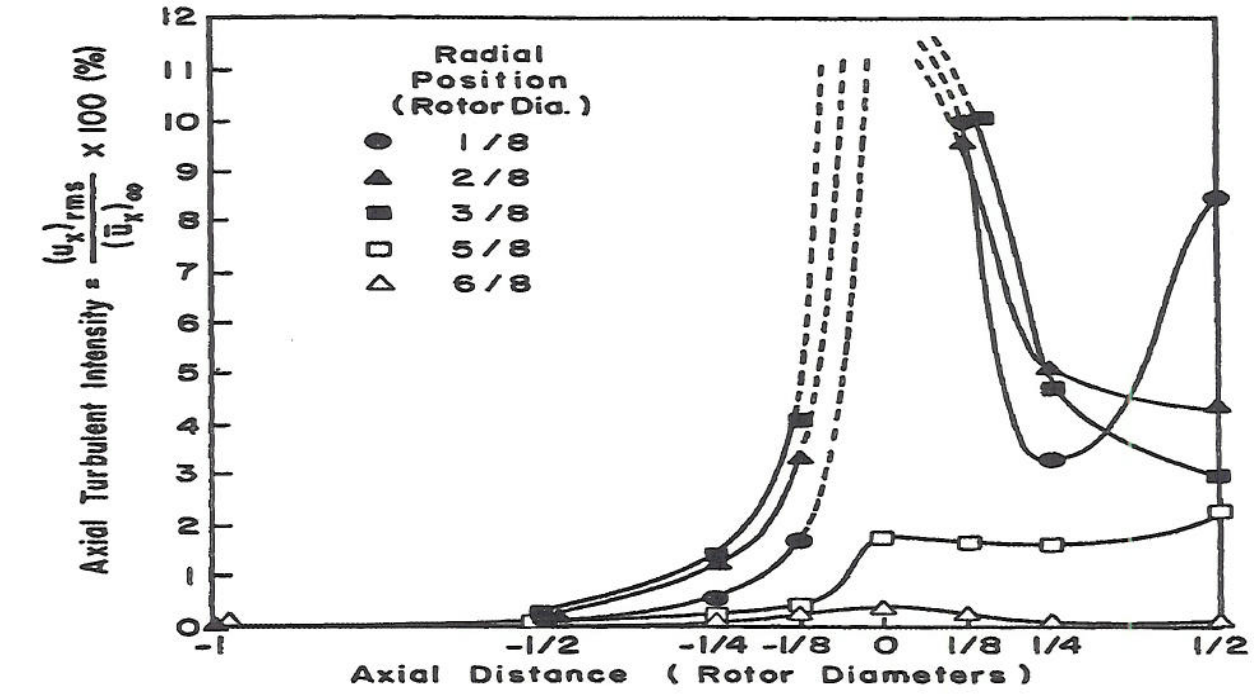

Figure 6 Axial turbulence intensity vs. axial distance for U = 7.6 m/s, T.I. = 0.1%